JOURNAL OF
Materials
CHEMISTRY

Tetrathiapentalene-based organic conductors with 1 : 1 composition

Mao Katsuhara,[a] Masanobu Aragaki,[a] Shinya Kimura,[a] Takehiko Mori,*[a] Yohji Misaki[b] and Kazuyoshi Tanaka[b]

[a]*Department of Organic and Polymeric Materials, Graduate School of Science and Engineering, Tokyo Institute of Technology, Meguro-ku, Tokyo 152-8552, Japan.*
E-mail: takehiko@o.cc.titech.ac.jp; Fax: +81-3-5734-2876; Tel: +81-3-5734-2427
[b]*Department of Molecular Engineering, Graduate School of Engineering, Kyoto University, Yoshida, Kyoto 606-8501, Japan*

Received 26th February 2001, Accepted 4th May 2001
First published as an Advance Article on the web 23rd May 2001

We have prepared TTM-TTP-based (TTM-TTP = 2,5-bis[4,5-bis(methylthio)-1,3-dithiol-2-ylidene]-1,3,4,6-tetrathiapentalene) organic conductors with 1 : 1 composition including tetrahedral anions in order to elucidate electronic properties of half-filled conductors. We have obtained three new 1 : 1 composition salts (TTM-TTP)$GaCl_4(PhCl)_{0.5}$, (TTM-TTP)$GaBr_4(PhCl)_{0.5}$, and (TTM-TTP)$GaBr_{2.0}Cl_{2.0}(PhCl)_{0.5}$, which have dimerized donor columns. (TTM-TTP)$GaCl_4(PhCl)_{0.5}$ shows paramagnetism in spite of the apparent band-insulating electronic structure. In addition we have obtained a metal alloy salt, (TTM-TTP)$Fe_{0.9}Ga_{0.1}Cl_4$. This salt has uniform donor columns and shows high electrical conductivity.

The study of organic conductors with inorganic magnetic counter anions has attracted a great deal of attention because of their intriguing physical properties. BETS-based (BETS = bis(ethylenedithio)tetraselenafulvalene) conducting salts with iron halides show many interesting properties, which seem to be derived from magnetic interaction between π-electrons on the donors and local spin moments on the Fe^{3+} ions.[1] The conducting properties of these salts are affected by alignment of the Fe^{3+} spins, and the magnitude of the π–d interaction changes depending on the counter anions and crystal structures. λ-$(BETS)_2FeCl_4$ undergoes an M–I transition at 8 K, which is brought about by antiferromagnetic (AF) order of Fe spins.[2] On the other hand, in κ-$(BETS)_2FeBr_4$, the superconducting state coexists with AF order of Fe spins below $T_{SC} = 1.1$ K.[3] Thus, the properties of organic conductors with magnetic anions are strikingly different from those of pure π systems. For the development of new organic conductors, it is important to explore the microscopic mechanism of the π–d interaction and to control the magnitude of the interaction.

From this viewpoint, we have reported TTM-TTP based organic conductors with 1 : 1 composition including magnetic anions, (TTM-TTP)$FeCl_4(PhCl)_{0.5}$, (TTM-TTP)$FeBr_4(PhCl)_{0.5}$, and (TTM-TTP)$FeCl_{2.2}Br_{1.8}$. The third salt is the first 1 : 1 composition *metallic* organic conductor with a magnetic anion.[4] In order to clarify the electronic state of donors in these materials, we have prepared TTM-TTP-based organic conductors including nonmagnetic anions with 1 : 1 composition; (TTM-TTP)$GaCl_4(PhCl)_{0.5}$, (TTM-TTP)$GaBr_4(PhCl)_{0.5}$, and (TTM-TTP)$GaCl_{2.0}Br_{2.0}(PhCl)_{0.5}$. In addition, we have found that alloying of the metal atoms gives the high conductivity phase, (TTM-TTP)$Fe_{0.9}Ga_{0.1}Cl_4$ as well. The present paper describes crystal structures and physical properties of these salts.

Results

Crystal and electric band structures

(TTM-TTP)$GaCl_4(PhCl)_{0.5}$, (TTM-TTP)$GaBr_4(PhCl)_{0.5}$, and (TTM-TTP)$GaCl_{2.0}Br_{2.0}(PhCl)_{0.5}$ are essentially isostructural (Fig. 1). These are also isostructural to the FeX_4 salts.[4] The crystallographic data are listed in Table 1. Unfortunately, in contrast to (TTM-TTP)$FeCl_{2.2}Br_{1.8}$, the halogen mixed salt (TTM-TTP)$GaCl_{2.0}Br_{2.0}(PhCl)_{0.5}$ does not have uniform columns, but is isostructural to the pure anion salts. The value of y in (TTM-TTP)$GaCl_{4-y}Br_y(PhCl)_{0.5}$ is determined from X-ray population analysis ($y = 2.0$) and EDS ($y = 2.0$), and these values show good agreement. Fig. 2 shows an ORTEP drawing of TTM-TTP in (TTM-TTP)$GaCl_4(PhCl)_{0.5}$. The shape of the molecule is almost planar except for one thiomethyl unit standing perpendicular to the molecular plane. The same has been observed in other TTM-TTP-based complexes whose donors are highly oxidized (+1). The central C=C bond lengths of TTM-TTP molecules (1.36(1), 1.31(5), 1.35(2) and 1.36(1) Å for the $GaCl_4^-$ salt, $GaBr_4^-$ salt, $GaCl_{2.0}Br_{2.0}^-$ salt, and $Fe_{0.9}Ga_{0.1}Cl_4^-$ salt, respectively) are consistent with those of other highly oxidized TTM-TTP-based salts (1.362(9) Å for (TTM-TTP)I_3).[5] A unit cell contains two donor molecules, two anions and a PhCl molecule that is incorporated from the solvent of the crystal growth. Hence the resulting composition is 1 : 1 : 0.5. A donor molecule is crystallographically independent, and located on a general position. The donor molecules make stacks in the crystallographic *c* direction (Fig. 1). Fig. 3 shows the overlap modes of the present salts. Because the donor molecules dimerize along the stacking direction, there are two overlap modes, c1 and c2. The interplanar spacing and the displacement of the donors are listed in Table 2. The columns of the present salts are made up of alternating stacks of ring-over-bond and 'ring-over-atom' overlaps (namely slid along the molecular short axis) (Fig. 3(b)). This is known as the β′-type structure in the ET (bis(ethylenedithio)tetrathiafulvalene) salts.[6] This structure contrasts with (TTM-TTP)AuI_2 and (TTM-TTP)$AuBr_2$, which are 1 : 1 composition organic conductors with linear anions.[7] The columns of the AuI_2^- and the $AuBr_2^-$ salts are composed of the usual ring-over-bond overlaps of the donor molecules (Fig. 3(a)). This corresponds to the β-type structure in the ET salts.[6] There are short S–S contacts between the donors in the same column, but those of the neighboring columns are only between outer thiomethyl groups, where π-electrons are not extended.

The GaX_4^- ions are located on general positions, and have

DOI: 10.1039/b101542g

This journal is © The Royal Society of Chemistry 2001

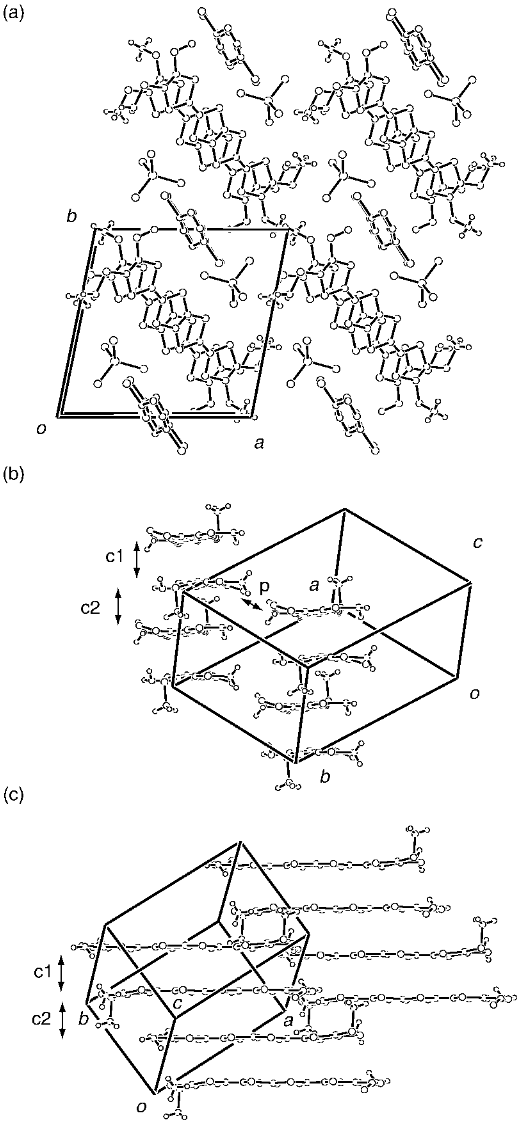

Fig. 1 The crystal structure of (TTM-TTP)$GaCl_4(PhCl)_{0.5}$. (a) Projection along the *c* axis, (b) view along the molecular short axis, and (c) view along the molecular long axis.

tetrahedral shape. The PhCl molecules are on inversion centers, and the position of Cl is disordered; the Cl atom is refined with 50% occupancy. There is no vacancy in the PhCl molecule, while the shape of PhCl is distorted to some extent. This is because the Cl atom has large temperature factors, and does not tend to be bonded to a definite carbon atom, indicating a large degree of freedom of the molecular rotation. Because these anions and solvent molecules exist between the donor chains, there are practically no interactions between the donor chains. Hence this system is regarded as highly one dimensional.

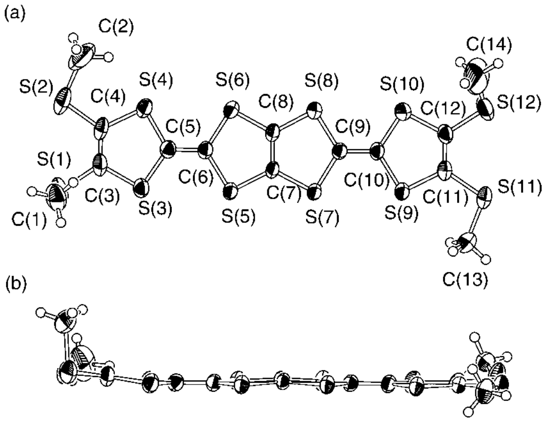

Fig. 2 (a) ORTEP drawing and atomic numbering scheme of TTM-TTP in the crystal of (TTM-TTP)$GaCl_4(PhCl)_{0.5}$ and (b) side view.

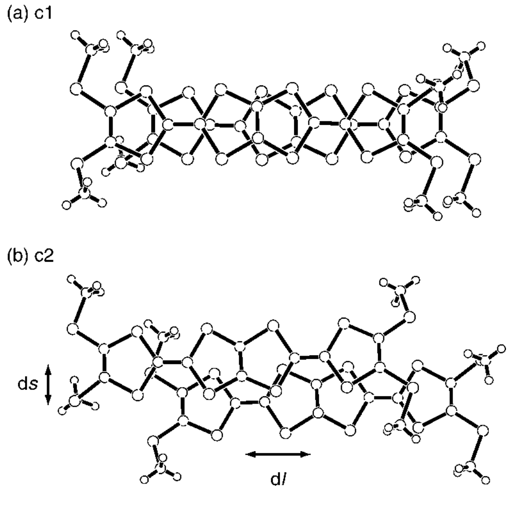

Fig. 3 Overlap modes of intrastack interactions of TTM-TTP in the crystal of (TTM-TTP)$GaCl_4(PhCl)_{0.5}$.

Table 1 Crystallographic data for (TTM-TTP)$GaCl_yBr_{4-y}(PhCl)_{0.5}$ and (TTM-TTP)$Fe_{0.9}Ga_{0.1}Cl_4$

	(TTM-TTP)$GaCl_4(PhCl)_{0.5}$ Rigaku AFC7R rt	(TTM-TTP)$GaCl_{2.0}Br_{2.0}(PhCl)_{0.5}$ Rigaku AFC7R rt	(TTM-TTP)$GaBr_4(PhCl)_{0.5}$ Rigaku AFC7R rt	(TTM-TTP)$Fe_{0.9}Ga_{0.1}Cl_4$ Rigaku AFC7R rt
Chemical formula	$C_{17}S_{12}H_{14.5}GaCl_{4.5}$	$C_{17}S_{12}H_{14.5}GaCl_{2.5}Br_2$	$C_{17}H_{14.5}S_{12}GaBr_4Cl_{0.5}$	$C_{14}H_{12}S_{12}Fe_{0.9}Ga_{0.1}Cl_4$
Formula weight	832.78	921.68	1010.58	764.11
Shape	Black needle	Black needle	Black needle	Black plate
Crystal system	Triclinic	Triclinic	Triclinic	Monoclinic
Space group	$P\bar{1}$	$P\bar{1}$	$P\bar{1}$	$C2/c$
a/Å	13.849(6)	14.136(2)	14.318(4)	24.021(7)
b/Å	14.215(8)	14.361(3)	14.507(4)	5.850(2)
c/Å	8.600(7)	8.571(1)	8.540(7)	22.435(7)
α/°	106.78(5)	105.88(1)	105.11(4)	90
β/°	94.77(5)	93.89(1)	93.16(4)	118.77(2)
γ/°	78.22(4)	76.65(1)	75.44(2)	90
V/Å^3	1586(2)	1628.3(5)	1657(1)	2764(2)
Z	2	2	2	4
D_{calc}/g cm^{-3}	1.743	1.880	2.025	1.836
λ/Å	0.71069	0.71069	0.71069	0.71069
Reflections used	4116 ($I > 5.00\sigma(I)$)	2421 ($I > 5.00\sigma(I)$)	2299 ($I > 5.00\sigma(I)$)	1510 ($I > 3.00\sigma(I)$)
R/R_w^{a}	0.065/0.071	0.070/0.090	0.115/0.153	0.049/0.052

$^a R = \Sigma\ \|F_o| - |F_c\|/\Sigma\ |F_o|$, $R_W = [\Sigma w\ (|F_o| - |F_c|)^2/\Sigma w\ F_o^2]^{1/2}$: $w = 1/\sigma^2$.

Table 2 The interplanar spacing and the displacement of the donors

	Mode	d*l*	d*s*	Interplanar spacing/Å
$(TTM\text{-}TTP)GaCl_4(PhCl)_{0.5}$	c1	1.56	0.10	3.38
	c2	3.33	1.91	3.46
$(TTM\text{-}TTP)GaCl_{2.0}Br_{2.0}(PhCl)_{0.5}$	c1	1.57	0.10	3.37
	c2	3.30	1.88	3.45
$(TTM\text{-}TTP)GaBr_4(PhCl)_{0.5}$	c1	1.58	0.15	3.35
	c2	3.29	1.82	3.48

The calculated overlap integrals of HOMO of the donors are listed in Table 3(a). In these materials, the Fermi energy is located between the energy bands as a result of the dimerized structure and the 1 : 1 composition. Accordingly the Fermi surface does not exist, suggesting that these salts are band insulators. The ratios of overlap integrals of c2 and c1, indicating the degree of dimerization, are around 0.2 and smaller than those of $(TTM\text{-}TTP)AuI_2$ and $(TTM\text{-}TTP)AuBr_2$ (about 0.7).[7] This demonstrates that the dimerization in the β′-type structure is much stronger than that in the β-type salts.

The metal alloyed compound, $(TTM\text{-}TTP)Fe_{0.9}Ga_{0.1}Cl_4$, has uniform donor columns and is almost isostructural to metallic mixed anion salts of iron halides, $(TTM\text{-}TTP)FeCl_{2.2}Br_{1.8}$[4] (Fig. 4). The crystallographic data of $(TTM\text{-}TTP)Fe_{0.9}Ga_{0.1}Cl_4$ is listed in Table 1. The donors are located on inversion centers and the MX_4^- ions are located on two-fold axes. The donors form a uniform stack along the *b* axis. Because the MX_4^- anions are located on the two-fold axes, two pairs of halogens are equivalent. The compositions of anions were determined from EDS, because it was difficult to determine the composition from population analysis on account of the small difference of electron numbers of Fe and Ga. The interplanar spacing of the donors is 4.76 Å and the displacement along molecular long axis is 3.40 Å. These values are the same as those in other 1 : 1 composition TTM-TTP-based organic metals with uniform columns, $(TTM\text{-}TTP)FeCl_{2.2}Br_{1.8}$,[4] $(TTM\text{-}TTP)I_3$[5] and $(TTM\text{-}TTP)[C(CN)_3]$.[8] Because of the highly one-dimensional donor columns, not only crystal and but also electronic structures of donor columns are considered to be almost the same.

The calculated overlap integrals are listed in Table 3(b). The overlap integrals between adjacent stacks are quite small, the ratio of intrastack and interstack overlap integrals are about 100 : 1, indicating high one-dimensionality. The Fermi surface, which is one-dimensional along the *b* axis, appears in spite of the 1 : 1 composition, because the column is uniform (Fig. 5). The Fermi surface is almost the same as that of $(TTM\text{-}TTP)FeCl_{2.2}Br_{1.8}$, $(TTM\text{-}TTP)I_3$[5] and $(TTM\text{-}TTP)[C(CN)_3]$.[8]

Electrical resistivity

Electrical resistivities of the present compounds are shown in Fig. 6.

Table 3 Overlap integrals (*S*) of (a) $(TTM\text{-}TTP)MCl_yBr_{4-y}(PhCl)_{0.5}$ and (b) $(TTM\text{-}TTP)Fe_{0.9}Co_{0.1}Cl_4$

	$S \times 10^{-3}$			
(a)	c1	c2	p1	c2/c1
$(TTM\text{-}TTP)GaCl_4(PhCl)_{0.5}$	28.8	−7.42	−0.02	0.26
$(TTM\text{-}TTP)GaCl_{2.0}Br_{2.0}(PhCl)_{0.5}$	30.1	−6.62	−0.03	0.22
$(TTM\text{-}TTP)GaBr_4(PhCl)_{0.5}$	30.4	−6.04	—	0.20

	$S \times 10^{-3}$	
(b)	b	p
$(TTM\text{-}TTP)Fe_{0.9}Ga_{0.1}Cl_4$	−20.9	0.18

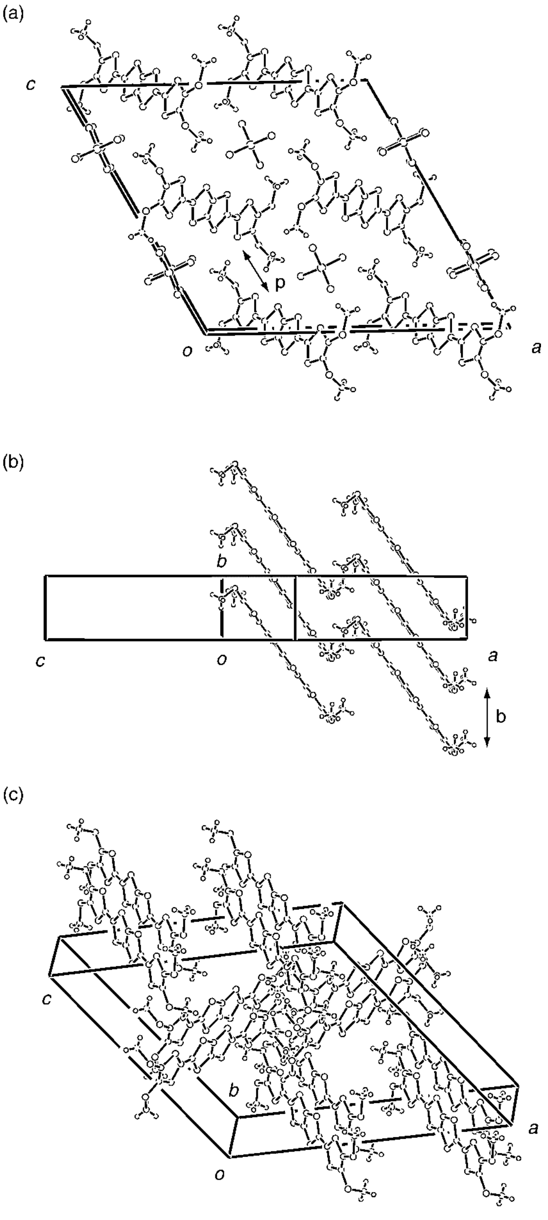

Fig. 4 The crystal structure of $(TTM\text{-}TTP)Fe_{0.9}Ga_{0.1}FeCl_4$. (a) Projection along the *b* axis, (b) structure of the columns, and (c) inclination of the donor molecules.

The dimerized salts show very low room-temperature conductivities (Table 4). These low values are related to the β′-type structure with strong dimerization. These salts are insulators even at room temperature. The activation energies are estimated from the temperature dependence of the electrical conductivity. These values are lower than the energy gap calculated from the band calculation (0.4 eV), but are almost the same as the activation energies of the FeX_4 salts (0.06 eV).[4]

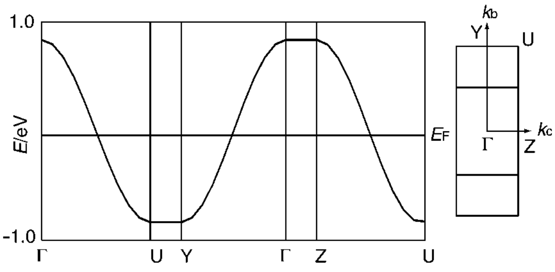

Fig. 5 Tight-binding energy band structures and Fermi surfaces of $(TTM\text{-}TTP)Fe_{0.9}Ga_{0.1}FeCl_4$.

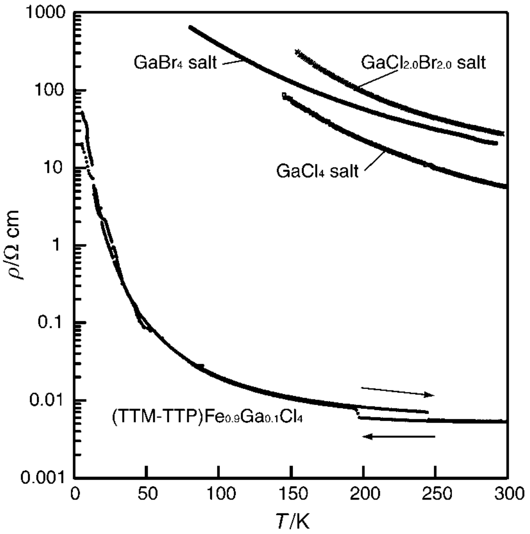

Fig. 6 Electrical resistivity of (TTM-TTP)$GaCl_{1-x}Br_x(PhCl)_{0.5}$ and (TTM-TTP)$Fe_{0.9}Ga_{0.1}FeCl_4$.

Furthermore, these values are also the same as those of (TTM-TTP)$AuBr_2$ and (TTM-TTP)AuI_2 (0.03 and 0.07 eV).[7]

(TTM-TTP)$Fe_{0.9}Ga_{0.1}Cl_4$ exhibits high room-temperature conductivity, and retains high conductivity down to about 200 K, below which this salt becomes an insulator. This behavior is similar to that of (TTM-TTP)$FeBr_{1.8}Cl_{2.2}$[4] and (TTM-TTP)I_3.[5]

Magnetic properties

Since strongly dimerized β′-salts with non magnetic anions are obtained in the first place, we have measured the static magnetic susceptibility and electron paramagnetic resonance of (TTM-TTP)$GaCl_4(PhCl)_{0.5}$ in order to make clear the electronic state of the π-system. Despite the insulating ground state corresponding to the strongly dimerized structure, the spin susceptibility is positive (Fig. 7), and does not change from room temperature to about 50 K, below which the susceptibility shows a Curie-like increase due to impurities. The magnitude of the spin susceptibility is comparable with that of metallic organic conductors such as $(TMTSF)_2AsF_6$.[9] Analogous behavior has been observed in a 1 : 1 composition organic conductor, (TTM-TTP)AuI_2, which has weaker dimerization than the present salts.[10]

The integrated intensity of the EPR, which is proportional to spin susceptibility, shows similar behavior (Fig. 8(a)). The g-value is consistent with that of the donor spins. The g-value and the linewidth do not show any striking changes in all temperature ranges (Fig. 8(b)). These results demonstrate a paramagnetic insulating state in spite of the apparently band-insulating energy band. One may like to attribute this puzzling paramagnetism to impurities. Similar activation energies of conductivity for (TTM-TTP)AuI_2 and the present salts seem to support this interpretation. We cannot, however, explain why susceptibility is not Curie-like but temperature independent. We cannot exclude an intrinsic interpretation similar to (TTM-TTP)AuI_2[10] that the paramagnetism comes from the correlation in a weakly dimerized band, even in the β′-salts.

Table 4 Electrical conductivity of (TTM-TTP)$GaCl_yBr_{4-y}(PhCl)_{0.5}$ and (TTM-TTP)$Fe_{0.9}Ga_{0.1}Cl_4$

	Column	σ_{rt}/S cm^{-1}	E_a/eV or T_{MI}/K
(TTM-TTP)$GaCl_4(PhCl)_{0.5}$	Dimerized β′	0.01	0.09 eV
(TTM-TTP)$GaCl_{2.0}Br_{2.0}(PhCl)_{0.5}$	Dimerized β′	0.03	0.07 eV
(TTM-TTP)$GaBr_4(PhCl)_{0.5}$	Dimerized β′	0.07	0.05 eV
(TTM-TTP)$Fe_{0.9}Ga_{0.1}Cl_4$	Uniform	190	200 K

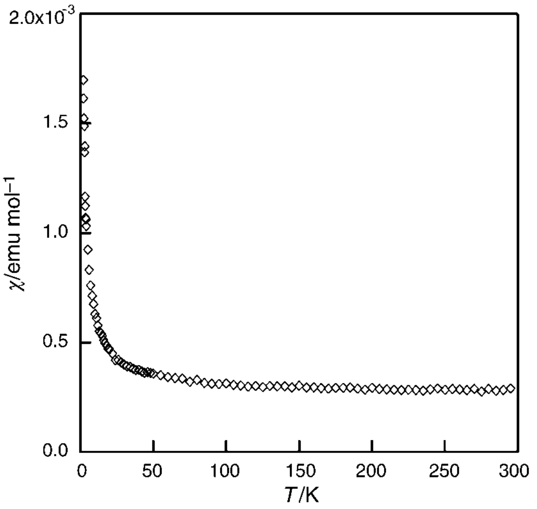

Fig. 7 Static magnetic susceptibility of (TTM-TTP)$GaCl_4(PhCl)_{0.5}$.

Fig. 9 shows the static magnetic susceptibility of (TTM-TTP)$Fe_{0.9}Ga_{0.1}Cl_4$. The susceptibility obeys the Curie–Weiss law from 300 to 2 K. The Curie constant of 4.5 K emu mol^{-1} is close to the value predicted for Fe^{3+}, while the Θ value (−1.5 K) indicates a very weak antiferromagnetic interaction between the Fe moments.

Conclusion

We have prepared new 1 : 1 composition TTM-TTP-based organic conductors with non-magnetic anions in order to

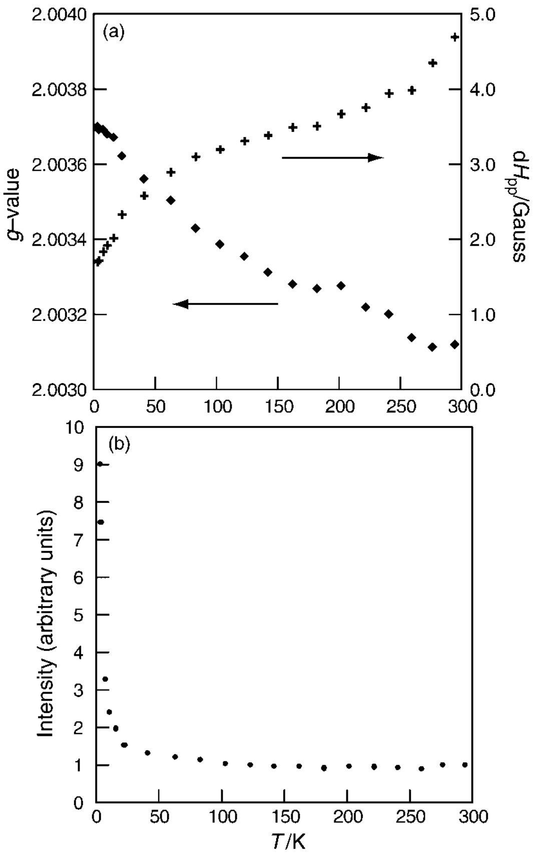

Fig. 8 (a) The g-value, peak-to peak linewidth and (b) normalized intensity of (TTM-TTP)$GaCl_4(PhCl)_{0.5}$.

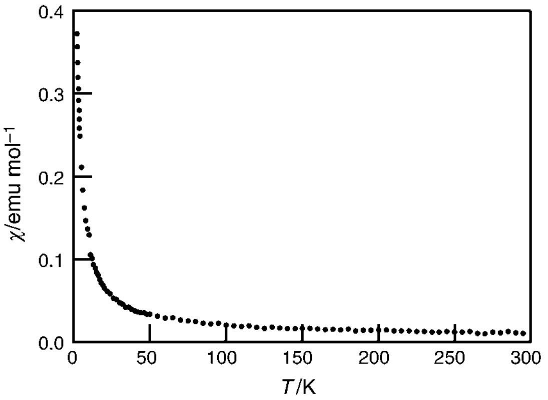

Fig. 9 Static magnetic susceptibility of (TTM-TTP)$Fe_{0.9}Ga_{0.1}Cl_4$.

clarify the electron state of π-systems in organic conductors with magnetic anions. We have obtained three new 1 : 1 composition TTM-TTP-based organic conductors with non-magnetic gallium halides, (TTM-TTP)$GaCl_4(PhCl)_{0.5}$, (TTM-TTP)$GaBr_4(PhCl)_{0.5}$, and (TTM-TTP)$GaCl_{2.0}Br_{2.0}(PhCl)_{0.5}$. In addition, we have prepared a metal alloyed salt, (TTM-TTP)$Fe_{0.9}Ga_{0.1}Cl_4$.

We have reported structures and properties of these salts. When we used pure GaX_4^-, as well as the mixture of $GaCl_4^-$ and $GaBr_4^-$, in electrocrystallization, we obtained the β′-type salts with dimerized columns, (TTM-TTP)$GaCl_4(PhCl)_{0.5}$, (TTM-TTP)$GaBr_4(PhCl)_{0.5}$, and (TTM-TTP)$GaCl_{2.0}Br_{2.0}$-$(PhCl)_{0.5}$. Reflecting the half-filled band and dimerized structure, these salts are insulators even at room temperature. The EPR results show that the spin degree of freedom in (TTM-TTP)$GaCl_4(PhCl)_{0.5}$ is not lost, in spite of the strongly dimerized structure, even when the charge mobility is lost. On the other hand, when we mixed metal anions in electrocrystallization, a high conductivity phase with uniform donor stacks, (TTM-TTP)$Fe_{0.9}Ga_{0.1}Cl_4$, was obtained. Not only halogen mixed salts, but also metal alloyed salts gave this uniform phase. This salt shows highly conductive behavior similar to other TTM-TTP-based salts with uniform donor columns. As a next step to stabilize the high conductivity state, we are now attempting to control the band filling in the uniform structure by alloying metal halides with different charges, M(III)Cl_4^- and M′(II)Cl_4^{2-}.

Experimental

Crystal growth

Crystals were grown by electrocrystallization in chlorobenzene in the presence of 2–3 mg of donor and 30–100 mg of tetrabutylammonium salts of the corresponding anions under a constant current of 0.5 μA at 26 °C using H-shaped cells with Pt electrodes. In the presence of pure GaX_4^- anion, and in a mixture of $TBAGaCl_4$ and $TBAGaBr_4$, crystals with a black needle shape, (TTM-TTP)$GaCl_4(PhCl)_{0.5}$, (TTM-TTP)-$GaBr_4(PhCl)_{0.5}$, and (TTM-TTP)$GaCl_{2.0}Br_{2.0}(PhCl)_{0.5}$ were obtained. When $TBAFeCl_4$ and $TBAGaCl_4$ were mixed, black plate crystals, (TTM-TTP)$Fe_{0.9}Ga_{0.1}Cl_4$ were obtained.

Although these salts contain non-stoichiometric anion mixtures, we could not control the composition continuously. Samples electrocrystallized by starting from different nominal anion ratios were investigated by EDS measurements and X-ray population analysis, giving a definite composition within experimental error. These samples showed similar conducting behavior as well. We considered that only the salts with these definite compositions are stable.

Structure determination

The crystal structures were determined from single crystal X-ray diffraction. Intensity data were measured by the ω scan technique on a Rigaku automated four-circle diffractometer AFC-7R with graphite monochromatized Mo-Kα radiation ($2\theta < 60°$), and the absorption effect was corrected empirically (ψ-scan method). The structures were solved by direct methods (SIR97[11]). The structures were refined by the full-matrix least squares procedure by applying anisotropic temperature factors for all non-hydrogen atoms.

CCDC reference numbers 159320–159323. See http://www.rsc.org/suppdata/jm/b1/b101542g/ for crystallographic files in .cif or other electronic format.

Electrical resistivity

Electrical resistivity was measured for single crystals by the four-probe method using a low-frequency ac current (usually 10 μA). Electrical contacts to the crystals were made with 15 μm gold wire and gold paint. The crystals were held in a cryostat, and cooled down to 1.5 K. To monitor the temperature a Cu–Constantan thermocouple and a carbon resistor sensor were used for above and below about 50 K, respectively.

Electron paramagnetic resonance (EPR)

Electron paramagnetic resonance spectra were measured with a conventional X-band spectrometer (JEOL JESS-TE200). Measurements of the present compounds were carried out for a single crystal. The magnetic field was applied approximately along the molecular long axis.

Static magnetic susceptibility

Measurements were performed using a Quantum Design SQUID magnetometer (MPMS-5) under $H = 10$ kOe. A polycrystalline sample was wrapped in a polyethylene sheet in a straw.

Electronic band structure

The overlap integrals of the highest occupied molecular orbital (HOMO) of the donors were estimated on the basis of the extended Hückel method, and then transfer integrals were estimated from overlap integrals of HOMOs.[12] Using these transfer integrals, the band calculation was carried out on the basis of the tight-binding approximation.

Acknowledgements

This work was partly supported by a Grant-in-Aid for Scientific Research on Priority Areas (B) of Molecular Conductors and Magnets (No. 11224203) from the Ministry of Education, Science, and Culture, Japan.

References

1 H. Kobayashi, A. Kobayashi and P. Cassoux, *Chem. Soc. Rev.*, 2000, **29**, 325.

2 H. Kobayashi, H. Tomita, T. Naito, A. Kobayashi, F. Sakai, T. Watanabe and P. Cassoux, *J. Am. Chem. Soc.*, 1996, **118**, 368.

3 E. Ojima, H. Fujiwara, K. Kato and H. Kobayashi, *J. Am. Chem. Soc.*, 1999, **121**, 5581.

4 M. Katsuhara, M. Aragaki, T. Mori, Y. Misaki and K. Tanaka, *Chem. Mater.*, 2000, **12**, 3186.

5 T. Mori, *Bull.Chem. Soc. Jpn.*, 1998, **71**, 2509.

6 T. Kawamoto, M. Aragaki, T. Mori, Y. Misaki and T. Yamabe, *J. Mater. Chem.*, 1998, **8**, 285.

7 T. Mori, H. Inokuch, Y. Misaki, T. Yamabe, H. Mori and S. Tanaka, *Bull. Chem. Soc. Jpn.*, 1994, **67**, 661; T. Mori, T. Kawamoto, J. Yamaura, T. Enoki, Y. Misaki, T. Yamabe, H. Mori and S. Tanaka, *Phys. Rev. Lett.*, 1997, **79**, 1702.

8 T. Mori, T. Kawamoto, K. Iida, J. Yamaura, T. Enoki, Y. Misaki, T. Yamabe, H. Mori and S. Tanaka, *Synth. Met.*, 1999, **103**, 1885.

9 K. Mortensen, Y. Tomokiewicz and K. Bechgaard, *Phys. Rev.*, 1982, **25**, 3319.

10 T. Kawamoto, T. Mori, T. Yamamoto, H. Tajima, Y. Misaki and K. Tanaka, *J. Phys. Soc. Jpn.*, 2000, **69**, 4066.

11 G. M. Sheldrick, in *Crystallographic Computing 3*, eds. G. M. Sheldrick, C. Kruger and R. Goddard, Oxford University Press, pp. 175, 1985.

12 T. Mori, A. Kobayashi, Y. Sasaki, H. Kobayashi, G. Saito and H. Inokuchi, *Bull. Chem. Soc. Jpn.*, 1984, **57**, 627.